LLNL-PROC-638986

Integration of FREYA into MCNP6. An Improved Fission Chain Modeling Capability.

J. M. Verbeke, C. A. Hagmann, J. Randrup, R. Vogt

June 13, 2013

INMM 2013 annual meeting
Palm Desert, CA, United States
July 14, 2013 through July 18, 2013

INTEGRATION OF FREYA INTO MCNP6: AN IMPROVED FISSION CHAIN MODELING CAPABILITY

J. M. Verbeke[1], C.A. Hagmann[1], J. Randrup[2], R. Vogt[1,3]
[1] Lawrence Livermore National Laboratory, P.O. Box 808, Livermore, CA 94551, USA
[2] Lawrence Berkeley National Laboratory, 1 Cyclotron Road, Berkeley, CA 94720, USA
[3] University of California, Davis, One Shields Avenue, Davis, CA 95616, USA

ABSTRACT

From nuclear materials accountability to detection of SNM, the need for better modeling of fission has grown over the past decades. Current radiation transport codes compute average quantities with great accuracy and performance, but performance and averaging comes at the price of limited interaction-by-interaction modeling. For fission applications, these codes often lack the capability of modeling interactions exactly: energy is not conserved, energies of emitted particles are uncorrelated, prompt fission neutron and gamma multiplicities are uncorrelated. Many modern applications require more exclusive quantities than averages, such as the fluctuations in certain observables (e.g. the neutron multiplicity) and correlations between neutrons and photons. The new computational model, FREYA (Fission Yield Event Yield Algorithm), aims to meet this need by modeling complete fission events. Thus it automatically includes fluctuations as well as correlations resulting conservation of energy and momentum. FREYA has been integrated into the LLNL fission library, which is an integral part of MCNP6. By comparing Monte Carlo simulations performed with and without the new fission model, we will see that the fluctuations and correlations introduced lead to significant differences that can be measured experimentally using detectors. The first part of this paper will focus on the new fission model FREYA and the LLNL fission library, while the second part will concentrate on results of simulations and comparisons to experimental data.

INTRODUCTION

Several general-purpose Monte Carlo codes (MCNP/X [1–5], TART [4, 6], COG [4, 7], GEANT [8], etc.) are currently available for modeling neutron transport. For fission, they have in common the "average fission model", which is characterized by outgoing projectiles (fission neutrons and gammas) that are uncorrelated and sampled from the same probability density function (pdf). This approximation is sufficient for the calculation of average quantities such as flux, energy deposition and multiplication. However it is unsuitable for studying detailed correlations between neutrons and/or gammas on an event-by-event basis. During the past decade several code extensions have been developed that allow the modeling of correlations in fission. MCNP-DSP [4, 9] and MCNPX-PoliMi [4, 10] added angular correlations of fission neutrons (using the ^{252}Cf spontaneous fission distribution for all fissionable nuclides). Both codes also include detailed multiplicity and energy distributions for prompt fission gammas time correlated with the fission event. A new option was introduced in MCNPX 2.7.0 [11] for the treatment of fission events utilizing a library developed at LLNL [12]. It features time-correlated sampling of gammas from neutron-induced fission, photofission and spontaneous fission. The correlations are however limited for these last 3 options (MCNP-DSP, MCNPX-PoliMi, LLNL Fission Library), as they sample outgoing particles from average fission distributions instead of sampling them from a single realization of a fission process. In recent years, various simulation treatments have made it possible to also address fluctuations of and correlations between fission observables. In particular, a Monte-Carlo approach was developed [13, 14] for the sequential emission of neutrons and gammas from individual fission fragments in binary fission. The more recent event-by-event fission model, FREYA, includes more fission isotopes and has been specifically designed for producing large numbers of fission events in a fast simulation [15–18]. Employing

(i) nuclear data for fragment mass and kinetic energy distributions,

(ii) statistical evaporation models for neutron and gamma emission,

(iii) conservation of energy and momentum,

these codes are able to predict a host of correlations between outgoing fission products. These include correlations in neutron multiplicity, energy and angles, and energy sharing between neutrons and gammas. In the present work, FREYA is used to provide samples of complete fission events. In order to model correlations in realistic detector arrays, we have integrated the standalone fission event generator FREYA into the LLNL fission library, which is an integral part of the transport codes MCNPX 2.7.0 and MCNP6. We are closely working with the developers of MCNP6 to produce a publicly available version of the code in the near future.

Of the possible correlations between outgoing fission products and emitted neutrons and gammas, only angular neutron correlations have been experimentally established [19–23]. In this paper, we will compare the results of the MCNPX 2.7.0/LLNL Fission Library/FREYA code combination with experimental results.

STATE-OF-THE-ART FISSION MODELS IN THE MCNP CODE FAMILY

The LLNL Fission Library [12] was first integrated into a beta release of MCNPX2.7.0 and it now available in MCNP6. At the time of its integration, several new features were added to MCNPX2.7.0.

SPONTANEOUS FISSION

The LLNL Fission Library introduced sampling of fission gammas for spontaneous fission to MCNPX, which only emitted fission neutrons prior to that. The number of fission gammas is sampled from multiplicity distributions taken from the literature or physics models [12, 24]. The energies of these fission gammas is also sampled from distributions taken from the literature [9, 12].

NEUTRON-INDUCED FISSION

Before the LLNL Fission Library was integrated into MCNPX, neutron-induced fissions were not producing time-correlated fission gammas. This is illustrated in Fig. 1: first a neutron would interact with a nucleus. Second, the code would emit a number of gammas. Third, MCNPX would determine what reaction took place before fourth, emitting fission-specific neutrons. The gammas were emitted before the code knew what reaction took place and were therefore not correlated to the reaction, but were instead taken from all possible gamma-producing reactions in both number and energy. To remedy this situation, the LLNL Fission Library moved the emission of fission gammas after the code determines which reaction occurred. Gammas are now nuclear reaction specific: Fission gammas are emitted when a fission reaction takes place, while other gammas are only produced when other nuclear reactions occur. For fission events, the Fission Library samples number and energy of gammas from published distributions [9, 12, 24].

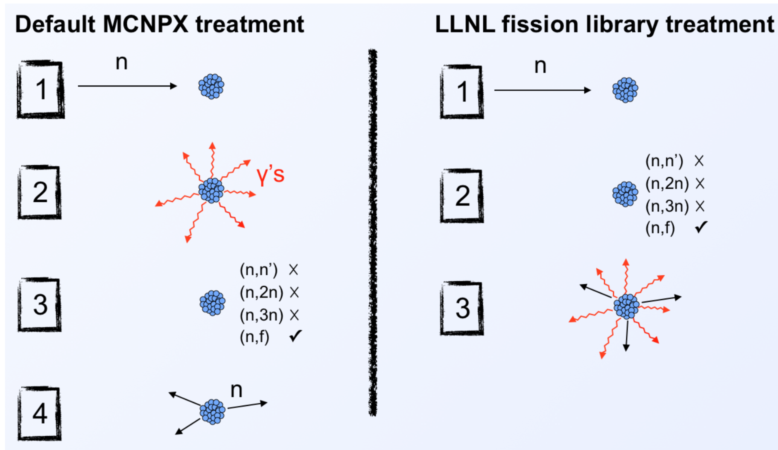

Figure 1: Comparison between LLNL Fission Library and default treatments in MCNPX2.7.0 for fission gamma multiplicity.

PHOTOFISSION

In the default MCNPX treatment shown in Fig. 2, a photon first interacts with a nucleus. Neutrons are then emitted before even knowing what photonuclear reaction took place. The code would actually never determine which photonuclear reaction took place, and emit reaction-aspecific neutrons. MCNPX did not emit any gammas in photonuclear reactions. With the LLNL fission library, the gamma first interacts with the nucleus, the photonuclear reaction is then determined, followed by emission of reaction-specific neutrons and gammas. In photofission, the outgoing secondary particles are photofission-specific and time-correlated with the photonuclear reactions.

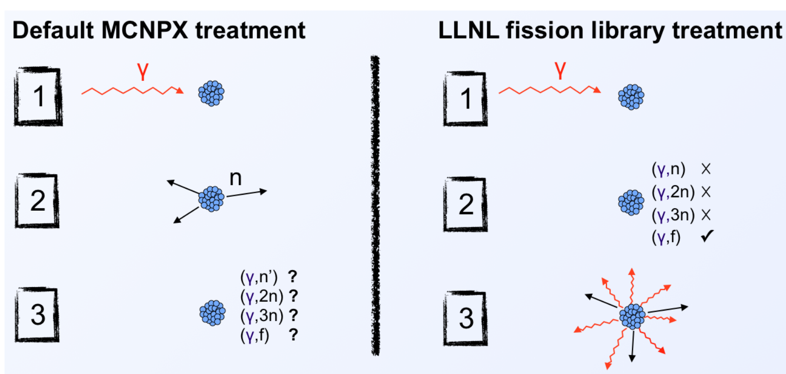

Figure 2: Comparison between LLNL Fission Library and default treatments in MCNPX2.7.0 photofission.

MODELING FISSION WITH FREYA

We start with a fissile nucleus ${}^{A_0}Z_0$ with excitation energy E_0^* that undergoes binary fission into a heavy ${}^{A_H}Z_H$ and a light fragment ${}^{A_L}Z_L$. The fragment masses are obtained from experimental mass yields $Y(A)$, see Ref. [15].

Once the mass and charge of the two fragments have been selected, the Q value of the fission channel is the difference between the total mass of A_0 and the fragment ground-state masses, $Q_{LH} = M(A_0) - M_L - M_H$.

The Q_{LH} value is divided between the total kinetic energy (TKE) and the total excitation energy (TXE) of the fragments. The average TKE is assumed to take the form $\overline{\mathrm{TKE}}(A_H, E_\mathrm{n}) = \overline{\mathrm{TKE}}_\mathrm{data}(A_H) + d\mathrm{TKE}(E_\mathrm{n})$. The first term is extracted from data while the second is adjusted to the measured average neutron multiplicity, $\overline{\nu}$.

After the average total fragment kinetic energy, $\overline{\mathrm{TKE}}$, has been sampled, the combined statistical fragment excitation energy, $\overline{\mathrm{TXE}}$, follows from energy conservation, $\overline{\mathrm{TXE}} = \overline{E}_L^* + \overline{E}_H^* \doteq Q_{LH} - \overline{\mathrm{TKE}}$.

If the fragments are in mutual thermal equilibrium, their temperatures are equal, $T_L = T_H$, and their statistical excitation energy is proportional to the level-density parameter, *i.e.* $\overline{E}_f^* \sim a_f$. FREYA first assigns average excitations, $\acute{E}_f^*$, based on such an equipartition, $\acute{E}_f^* = a_f(\tilde{E}_f^*)\overline{\mathrm{TXE}}/(a_L(\tilde{E}_L^*) + a_H(\tilde{E}_H^*))$ where $\tilde{E}_f^* = (A_f/A_0)\overline{\mathrm{TXE}}$. (The value of the asymptotic level density parameter, e_0, is obtained from the ^{239}Pu evaluation [18] and is assumed to be universal.) Subsequently, because the observed neutron multiplicities suggest that the light fragments are more excited (probably due to their greater distortion at scission), the average excitations are adjusted as $\overline{E}_L^* = x\acute{E}_L^*$, $\overline{E}_H^* = \overline{\mathrm{TKE}} - \overline{E}_L^*$, where $x > 1$ is a parameter.

After the mean excitation energies have been assigned, FREYA accounts for thermal fluctuations. The fragment temperature T_f is obtained from $\overline{U}_f \equiv U_f(\overline{E}_f^*) = a_f T_f^2$, where $U(E^*) = E^*$. The variance in the excitation E_f^* is then $\sigma_f^2 = 2\overline{U}_f^* T_f$. Therefore, for each of the two fragments, we sample a thermal fluctuation δE_f^* from a normal distribution of variance σ_f^2 and modify the fragment excitation energies as, $E_f^* = \overline{E}_f^* + \delta E_f^*$. Energy conservation causes a compensating fluctuation in TKE leading to $\mathrm{TKE} = \overline{\mathrm{TKE}} - \delta E_L^* - \delta E_H^*$ [18].

Neutron evaporation occurs after the fragments have reached their asymptotic velocities. For a fragment of statistical excitation E^*, the maximum temperature in its evaporation daughter, T_max, is obtained from $aT_\mathrm{max}^2 = E^* - S_n(Z,A)$, where $S_n(Z,A)$ is the neutron separation energy. The neutron kinetic energy ε is sampled from $f_n(\varepsilon) \sim \varepsilon \exp(-\varepsilon/T_\mathrm{max})$. Neutrons are emitted as long as the Q value for emission exceeds $E_{n\mathrm{cut}}$ where photon emission takes over.

After neutron evaporation has ceased, the residual product nucleus has a statistical excitation energy of $E^* < S_n(Z,A) + E_{n\mathrm{cut}}$ and de-excites by sequential statistical gamma emission. Statistical photon emission is treated analogous to neutron evaporation except there is no separation energy for gammas. Since the gammas are massless, we introduce an infrared cut-off energy. Furthermore, there is an extra energy factor in the gamma phase space, $f_\gamma(E) \sim E^2 \exp(-E/T)$ where T, nuclear temperature prior to emission is equal to the maximum possible temperature after emission. Gammas are emitted isotropically in the frame of the emitter nucleus. Emission continues until the available statistical excitation energy has been exhausted.

FREYA CODE INTEGRATION

FREYA was first integrated into the LLNL Fission Library, which already provided an existing interface to MCNPX and MCNP6. Conveniently, no modification of MCNPX/MCNP6 was necessary after the LLNL Fission Library was substituted in the source code tree.

Upon startup, MCNP reads in a master FREYA data file containing

(1) the ZA of the available compound nuclei before fission. There are currently 7 fissionable isotopes: 4 spontaneous fission isotopes (^{238}U, ^{240}Pu, ^{244}Cm, ^{252}Cf), and 3 neutron-induced isotopes (^{233}U, ^{235}U, ^{239}Pu),

(2) the maximum numbers of pre-fission neutrons in multi-chance fission,

(3) the names of the FREYA data files containing

   (a) the probability distributions of mass partition $P(A_f)$,

   (b) the pre-equilibrium emission probabilities,

   (c) the pre-equilibrium emission spectra,

(d) the kinetic energy distributions of the fission fragments.

Because additional isotopes are expected to be regularly added in the future, the code was designed to ease the extension to additional isotopes: algorithm and data are completely separated and isotopes can easily be added by adding lines to the master FREYA data file, and generating some of the required files 3a through 3d listed in the enumeration above.

Currently, FREYA selects outgoing projectiles from spontaneous and neutron-induced fission for neutron energies below 20 MeV. Photofission is planned for the near future. For each spontaneous or neutron-induced fission event, the code checks whether the sampled isotope is available in FREYA. If present, FREYA is called to sample multiplicity, energy, and direction of the fission neutrons, all of which are passed back to the LLNL Fission Library and eventually to MCNP for transport. All other fission events are handled by the default LLNL fission library settings in the usual way. When in use, FREYA predicts a host of correlations between outgoing fission products: correlations in neutron multiplicity, energy and angles, and energy sharing between neutrons and gammas.

We verified [25] that FREYA is yielding the correct average neutron induced fission spectrum within MCNP by calculating the criticality parameter k_{eff} for the critical assemblies Godiva and Jezebel [26]. The k_{eff} results using FREYA were 0.9994 ± 0.0009 (Jezebel) and 1.0003 ± 0.0008 (Godiva), in good agreement with the default MCNP values.

FISSION-NEUTRON ANGULAR CORRELATIONS

Angular correlations between fission neutrons have been measured in the past [20–23]. Almost all of the neutrons in spontaneous and low energy fission are emitted by the fully accelerated fission fragments whose back-to-back motion is imprinted on the neutron directions in the laboratory frame. Thus small angle correlations are expected from neutrons emitted from the same fragment, whereas large angle correlations arise from opposite fragments. FREYA evaporates neutrons isotropically in the center-of-mass system of the fragments and boosts them back into the laboratory frame resulting in angular correlations. We will compare these fission neutron angular correlations for both experimental data and simulation.

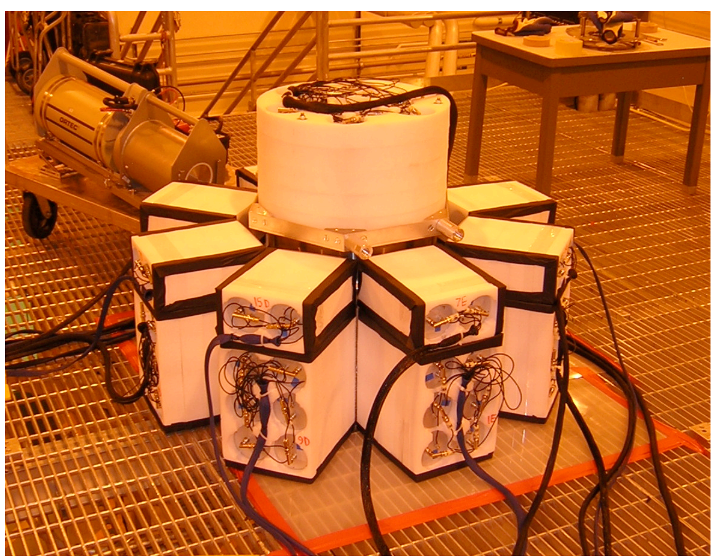

Figure 3: Photograph of the 77-cell liquid scintillator array.

EXPERIMENTAL RESULTS

A photograph of our detection system is shown in Fig. 3. The detector consists of 77 xylene cells, each read out by a single photomultiplier tube. Each tower of 8 cells is symmetrically arranged into octants with an array inner diameter of 60 cm. 13 identical cells compose the top of the detection system. The detector was designed for fast multiplicity counting and assaying of fissile material. The fast scintillator decay time of a few ns allows faster count rates than ^{3}He well counters. The relatively tightly-packed system has an overall geometric efficiency of 50% (2π).

The cells of the liquid scintillator array were calibrated in energy using the Compton edge of a ^{137}Cs source [27]. Neutron-gamma separation is accomplished by pulse shape discrimination (PSD), and was optimized using a ^{252} Cf source [28]. Separation is very good for neutrons with energies greater than 1 MeV, and degrades below that energy. The overall detection efficiency for unmoderated fission neutrons from ^{240}Pu was calculated to be approximately 7%. Since timing is important for any time-sensitive correlations, ^{137}Cs data were used to synchronize all the cells to sub-nanosecond time resolution using a Compton scattering algorithm [29].

Placing a 230 μCi ^{252}Cf source in the center of the detection system for approximately 30 minutes, we measured the angular correlation between fission neutrons emitted. Two neutrons are assumed to be of the same spontaneous fission if they are detected within 40 ns of each other. The angular correlation shown in red in Fig. 4 shows the anisotropy in the angular correlation as a function of μ, the direction cosine of the angle between the 2 neutrons.

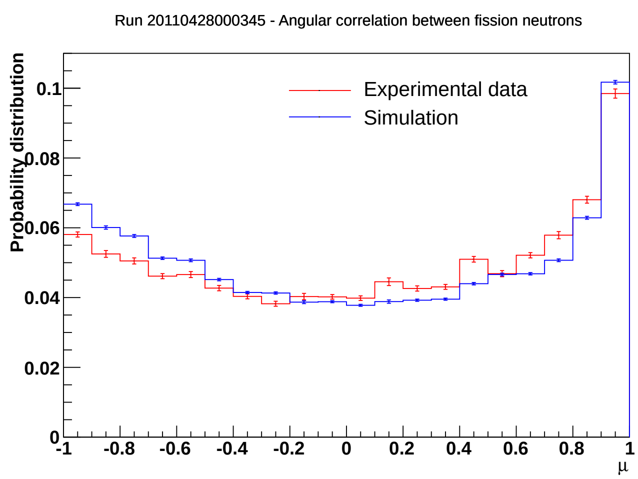

Figure 4: Angular correlation between ^{252}Cf spontaneous fission neutrons measured experimentally (red, 30 minutes of experimental data) and calculated using MCNP2.7.0/LLNL Fission Library/FREYA (blue, 3 minutes of simulated data).

While literature [20, 23] indicated a quasi-symmetric angular distribution, our experimental data shows a distribution that peaks in the forward direction. The analysis below will show that this is the result of multiple scattering. Indeed, while neutrons are captured in ^{3}He tubes, they survive their scattering with protons in liquid scintillator cells, and have a chance to be recorded a second or even a third time in other cells, even though this probability becomes lower and lower as they lose energy.

SIMULATION RESULTS

To reproduce the angular correlation experimentally measured, we used a MCNPX detector model developed for the large array of liquid scintillators shown in Fig. 3. Fig. 5 depicts the detector configuration. Using

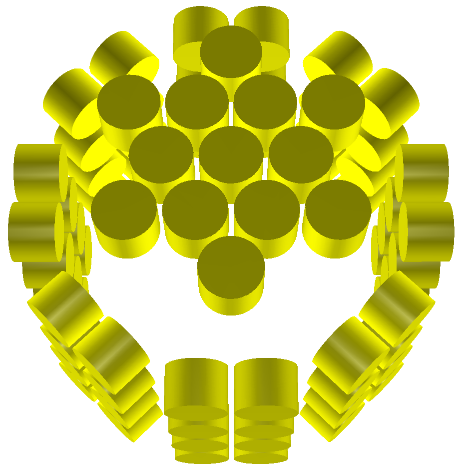

Figure 5: Model of the 77 liquid scintillator array.

MCNPX with FREYA turned on, we ran a simulation which produced the angular correlation shown in blue in Fig. 4. While the two distributions do not match perfectly, the FREYA model reproduces qualitatively the experimental data. Without FREYA, the distribution would be flat.

To study the effect of multiple scattering in liquid scintillators, we modified the simulation in such a way that neutrons are terminated after their first scattering in the liquid scintillator cells, suppressing hence any possibility of any neutron registering multiple counts. The results of this study are shown in Fig. 6. When multiple scattering is turned off, the peak at $\mu = 1$ completely vanishes and we obtain the expected more symmetric distribution in magenta.

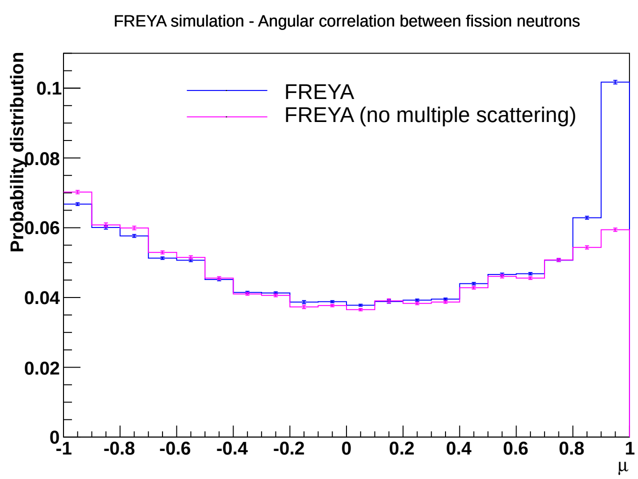

Figure 6: Effect of multiple scattering in liquid scintillator cells.

CONCLUSION

We have integrated the event-by-event fission generator FREYA into the LLNL fission library, which is an integral part of MCNPX2.7.0 and MCNP6. This new capability enables the simulation of correlations that are not predicted by conventional neutron Monte Carlo codes. Neutron angular correlations have been documented in the past and were recently measured by means of an array of liquid scintillators. They provide a tell-tale signature of fission and would be useful for the rejection of cosmic neutrons in SNM detectors.

Several improvements of FREYA are planned, such as a more refined treatment of fission gammas and the addition of more isotopes. We are working with the MCNP team at LANL to make FREYA publicly available to the wider community within MCNP6. It will also be made available to the GEANT4 community in the longer term.

ACKNOWLEDGMENTS

This work performed under the auspices of the U.S. Department of Energy by Lawrence Livermore National Laboratory under Contract DE-AC52-07NA27344.

References

[1] X-5 Monte Carlo Team, "MCNP A General Monte Carlo N-Particle Transport Code, Version 5 - Volume I: Overview and Theory," Los Alamos National Laboratory, Los Alamos, NM, LA-UR-03-1987 (2008). 1

[2] X-5 Monte Carlo Team, "MCNP A General Monte Carlo N-Particle Transport Code, Version 5 - Volume II: User's Guide," Los Alamos National Laboratory, Los Alamos, NM, LA-CP-03-0245 (2003). 1

[3] X-5 Monte Carlo Team, "MCNP A General Monte Carlo N-Particle Transport Code, Version 5 - Volume III: Developer's Guide," Los Alamos National Laboratory, Los Alamos, NM, LA-CP-03-0284 (2003). 1

[4] Available from the Radiation Safety Information Computational Center, http://rsicc.ornl.gov. 1

[5] T. Goorley et al. "Initial MCNP6 Release Overview - MCNP6 version 1.0," Los Alamos National Laboratory, Los Alamos, NM, LA-UR-13-22934 (2013). 1

[6] D. E. Cullen, "TART2005: A Coupled Neutron-Photon 3-D, Combinatorial Geometry, Time Dependent Monte Carlo Transport Code," Lawrence Livermore National Laboratory, Livermore CA, UCRL-SM-218009 (2005). 1

[7] R.M. Buck and E. M. Lent, "COG Users Manual: A Multiparticle Monte Carlo Transport Code," Lawrence Livermore National Laboratory, Livermore CA, UCRL-TM-202590, 5^{th} Edition (2002). 1

[8] Available from the European Organization for Nuclear Research, http://geant4.cern.ch. 1

[9] T. E. Valentine, "MCNP-DSP Users Manual," Oak Ridge National Laboratory, Oak Ridge, TN, ORNL/TM-13334 R2 (January 2001). 1, 2

[10] E. Padovani, S. A. Pozzi, S. D. Clarke and E. C. Miller, "MCNPX-PoliMi Users Manual," C00791 MNYCP, Radiation Safety Information Computational Center, Oak Ridge National Laboratory (2012). 1

[11] D. B. Pelowitz, J. W. Durkee, J. S. Elson, M. L. Fensin et al., "MCNPX 2.7.0 Extensions," Los Alamos National Laboratory, Los Alamos, NM, LA-UR-11-02295 (2011). 1

[12] J. M. Verbeke, C. Hagmann and D. Wright, "Simulation of Neutron and Gamma-Ray Emission from Fission and Photofission," Lawrence Livermore National Laboratory, Livermore CA, UCRL-AR-228518, Lawrence Livermore National Laboratory (2010). 1, 2

[13] S. Lemaire, P. Talou, T. Kawano, M. B. Chadwick and D. G. Madland, "Monte Carlo approach to sequential neutron emission from fission fragments," Phys. Rev. C, vol. 72, pp. 024601-1-12 (2005). 2

[14] S. Lemaire, P. Talou, T. Kawano, M. B. Chadwick and D. G. Madland, "Monte Carlo approach to sequential γ-ray emission from fission fragments," Phys. Rev. C, vol. 73, pp. 014602-1-9 (2006). 2

[15] J. Randrup and R. Vogt, "Calculation of fission observables through event-by-event simulation," Phys. Rev. C, vol. 80, pp. 024601-1-11 (2009). 2, 3

[16] R. Vogt, J. Randrup, J. Pruet and W. Younes, "Event-by-event study of prompt neutrons from ^{239}Pu(n,f)," Phys. Rev. C, vol. 80, pp. 044611-1-16 (2009). 2

[17] R. Vogt and J. Randrup, "Event-by-event study of neutron observables in spontaneous and thermal fission," Phys. Rev. C, vol. 84, pp. 044612-1-14 (2011). 2

[18] R. Vogt, J. Randrup, D. A. Brown, M. A. Descalle and W. E. Ormand, "Event-by-event evaluation of the prompt fission neutron spectrum from ^{239}Pu(n,f)," Phys. Rev. C, vol. 85, pp. 024608-1-18 (2012). 2, 4

[19] S. Debenedetti, J. E. Francis, Jr., W. M. Preston and T. W. Bonner, "Angular dependence of coincidences between fission neutrons," Phys. Rev., vol. 74, pp. 1645-1650 (1948). 2

[20] H. R. Bowman, S. G. Thompson, J. C. Milton and W. J. Swiatecki, "Velocity and angular distributions of prompt neutrons from spontaneous fission of ^{252}Cf," Phys. Rev., vol. 126, pp. 2120-2136 (1962). 2, 5, 6

[21] J. S. Pringle and F. D. Brooks, "Angular correlation of neutrons from spontaneous fission of ^{252}Cf, Phys. Rev. Lett., vol. 35, pp. 15631566 (1975). 2, 5

[22] C. B. Franklyn, C. Hofmeyer and D. W. Mingay, Angular correlation of neutrons from thermal-neutron fission of ^{235}U, Phys. Lett. B, vol. 78, pp. 564-567 (1978). 2, 5

[23] C. Budtz-Jørgensen and H.-H. Knitter, "Simultaneous investigation of fission fragments and neutrons in ^{252}Cf (sf)," Nucl. Phys. A, vol. 490, pp. 307-328 (1988). 2, 5, 6

[24] G.S. Brunson, Jr., "Multiplicity and Correlated Energy of Gamma Rays Emitted in the Spontaneous Fission of Californium-252," Ph.D. Thesis, University of Utah (1982). 2

[25] C. Hagmann, J. Randrup and R. Vogt, "FREYA A new Monte Carlo code for improved modeling of fission chains," Trans. Nucl. Sci., vol. 60, pp. 545-549 (2013). 5

[26] International Handbook of Evaluated Criticality Safety Benchmark Experiments, NEA Nuclear Science Committee (2007), http://icbep.inel.gov. 5

[27] J. M. Verbeke and S. Ouedraogo, "Calibration of Liquid Scintillators: I. Energy Calibration," Lawrence Livermore National Laboratory, Livermore CA, LLNL-TR-639553, Lawrence Livermore National Laboratory (2013). 6

[28] J. M. Verbeke and S. Ouedraogo, “Calibration of Liquid Scintillators: II. Sigmalization Approach to Pulse Shape Discrimination,” Lawrence Livermore National Laboratory, Livermore CA, LLNL-TR-612312, Lawrence Livermore National Laboratory (2013). 6

[29] J. M. Verbeke and S. Ouedraogo, “Calibration of Liquid Scintillators: III. Clock Synchronization Between Cells,” Lawrence Livermore National Laboratory, Livermore CA, LLNL-TR-, Lawrence Livermore National Laboratory (2013). 6

[30] J. M. Verbeke, L. Nakae, P. Kerr, D. Dietrich and A. Dougan, “Testing of liquid scintillator materials for gamma and neutron detection,” proceedings of the INMM conference, Tucson, AZ, Jul. 14-15, 2009, LLNL-CONF-414602 (2009).